Acta Crystallographica Section B
Structural Science
ISSN 0108-7681

Anti-$KSbF_6$ structure of $CaTbF_6$ and $CdTbF_6$: a confirmation of the singular crystal chemistry of Tb^{4+} in fluorides

Michaël Josse, Marc Dubois, Malika El-Ghozzi, Joël Cellier and Daniel Avignant*

Université Blaise Pascal, Laboratoire des Matériaux Inorganiques, UMR 6002 CNRS, 24 Avenue des Landais, 63177 Aubiere, France

Correspondence e-mail: avignant@chimtp.univ-bpclermont.fr

Received 4 July 2004
Accepted 25 October 2004

The crystal structures of two new tetravalent terbium fluorides, $CaTbF_6$ and $CdTbF_6$, have been determined from X-ray and neutron powder diffraction data. The title compounds exhibit an *anti*-$KSbF_6$ structure, the three-dimensional framework of which is built of $[TbF_6]^{2-}$ chains of edge-sharing dodecahedra further linked, by sharing corners, to isolated $[MF_6]^{4-}$ octahedra (M = Ca, Cd). The mechanism of the anionic sublattice rearrangement when going from $KSbF_6$ to $CaTbF_6$ is described and related to a simple cubic fluoride-ion packing. Comparison with the crystal structures of β-$BaTbF_6$ and other representatives of the $M^{II}M'^{IV}F_6$ family allows the singular crystal-chemical properties of some fluoroterbates to be emphasized.

1. Introduction

Owing to their potential applications in various fields, such as optical or magnetic materials for instance, the crystal-chemical and physical properties of rare-earth oxides and fluorides have been extensively investigated for many years. If the physico-chemical properties of the rare earths in these materials are generally concerned with Ln^{3+} ions, the occurrence of other oxidation states (*e.g.* +2 and +4 for a few of them) frequently results in strong modifications of these properties. Comprehensive studies of the crystal chemistry of tetravalent lanthanides are then of the highest interest, as they can help to understand the role of Pr^{4+} or Tb^{4+} ions in supraconductors or phosphors, respectively. Previous results have already provided evidence of the singular crystal-chemical behavior of the Li_2TbF_6 representative within the $Li_2M^{IV}F_6$ series and emphasized the role of the half-filled shell of the $4f^7$ electronic configuration of the Tb^{4+} ion (Guillot *et al.*, 1992). Previous results in this field correlated the crystal chemistry of fluoroterbates with those of the fluorozirconates and fluorouranates through an empirical rule that points out the strong propensity of the Tb^{4+} ion for the eight-coordination in fluorides (El-Ghozzi & Avignant, 2001). An exception to this rule is provided by the series M_3TbF_7 (M = K, Rb, Cs; Feldner & Hoppe, 1983), the structures of which are closely related to the $(NH_4)_3ZrF_7$ type (Hurst & Taylor, 1970*a*,*b*). Apart from this example the only case where Tb^{4+} ions have not been found in eight-coordination in fluorides is in the mixed-valence terbium fluoride $Rb_2AlTb_3F_{16}$ (Josse *et al.*, 2003), where Tb^{3+} and Tb^{4+} ions are randomly distributed over a unique nine-coordinated crystallographic site. Other mixed-valence terbium fluorides have also recently been structurally characterized, either with a random Tb^{3+}/Tb^{4+} cationic distribution such as $RbAl_2Tb_4F_{22}$

(Josse *et al.*, 2005) or with long-range ordering such as KTb_3F_{12} (Largeau *et al.*, 1998) or $K_2Tb_4F_{17}$ (Largeau, 1998). In any case, all the terbium sites, either ordered Tb^{4+} and Tb^{3+} or mixed Tb^{3+}/Tb^{4+} sites, are eight-coordinated by the fluoride ions. The necessity of carrying out an additional structural characterization of the M_3TbF_7 (M = K, Rb, Cs) fluorides and the existence of a statistical distribution in the $Rb_2AlTb_3F_{16}$ fluoride imply that these two examples are not strictly inconsistent with the general trend (eight-coordination of the Tb^{4+} ion) observed in tetravalent terbium fluorides.

Thus, the main outstanding feature resulting from these studies is the eight-coordination always observed for Tb^{4+} ions in fluorinated environments, emphasizing the strong propensity of the Tb^{4+} ion for this coordination. Therefore, the leading idea for forthcoming work in this field is the research of counter-examples (if any) which is really inconsistent with the aforementioned empirical rule.

The title compounds were in evidence during previous investigations of the phase relationships in MF_2–TbF_4 systems (Largeau & El-Ghozzi, 1998). This paper deals with their crystal structure determination from high-resolution X-ray and neutron powder diffraction. Structural relationships with other hexahalides are also presented and discussed.

2. Experimental

The reagents were commercial CaF_2, CdF_2 (Merck selectipur) and TbF_4. Terbium tetrafluoride was prepared by fluorination of the Tb_4O_7 oxide (Strem chemical) at 773 K overnight under a pure fluorine gas flow. Polycrystalline samples of $CaTbF_6$ and $CdTbF_6$ have been obtained by heating overnight stoichiometric mixtures of CaF_2 + TbF_4 and CdF_2 + TbF_4, under pure fluorine gas flow at 923 and 723 K, respectively. The resulting powders were ground and annealed for 12 h in the same conditions to improve their crystallinity.

X-ray powder diffraction data were recorded on a Philips X'Pert Pro high-resolution powder diffractometer using graphite-monochromated Cu $K\alpha$ radiation, with an incident beam mask of 15 mm. The samples were put in a 16 mm diameter standard holder spinning at 3.75 r.p.m. Programmable divergence and anti-scattering slits, set for an irradiated length of 5.0 mm, were used. The programmable receiving slit aperture was set to 0.05°. The diffraction patterns were recorded over the 2θ angular range 5–140° with a step of 0.012° (2θ) and a counting time of 31 and 27 s per step for $CaTbF_6$ and $CdTbF_6$, respectively. The final patterns were converted to 'fixed slits' data, using the conversion algorithm, which is proportional to $1/\sin\theta$. This is available in the software package of the Philips X'Pert Pro diffractometer.

The neutron powder diffraction data of $CaTbF_6$ were recorded on the same sample, at room temperature, on a two-axis high-resolution 3T2 diffractometer (λ = 1.2251 Å; Roisnel *et al.*, 1994) at the Léon Brillouin Laboratory (Saclay, France). The pattern was recorded over the 2θ range 6–125° with a 2θ step of 0.05°. The strong absorption cross section (20 600 barns) of the ^{113}Cd isotope (natural abundance 12.22%) excluded the neutron data collection on $CdTbF_6$ in the experimental conditions available on the 3T2 instrument.

The $CaTbF_6$ and $CdTbF_6$ powder patterns exhibit very similar sequences of Bragg peaks, suggesting these compounds are isotypic. A few weak impurity peaks distinguishable in the X-ray diffraction patterns by their broad shape were observed, the most significant lines being located around $2\theta \simeq 26°$. The neutron diffraction pattern recorded on $CaTbF_6$ confirmed that these peaks were not assignable to a superstructure relating to the anionic sublattice as they were almost undetectable, although the anionic contribution to neutron diffraction predominates owing to the anion-rich stoichiometry investigated and the enhanced contrast offered by neutron diffraction (Finney, 1995).

3. Determination of the structure and refinement

In order to determine the structure of the title compounds, investigations were carried out on $CaTbF_6$, for which both X-ray and neutron powder data sets were available.

The X-ray powder diffraction pattern of $CaTbF_6$ was indexed using the program *WINDIC*, a windows-compliant version of *DICVOL91* (Boultif & Louër, 1991), from the first 20 lines, with an absolute error of 0.03° (2θ) leading to the following solution:

Tetragonal symmetry: a = 5.2677 (3), c = 7.7066 (9) Å, V = 213.85 Å^3, Bravais lattice P, Z = 2, M_{20} = 112.5, F_{20} = 95.5 (0.0068, 31).

The Miller indices of the Bragg peaks extracted from a 'pattern-matching' refinement of the X-ray powder diffraction pattern of $CaTbF_6$, performed with the *FULLPROF* program (Rodriguez-Carvajal, 1991), were carefully examined and confirmed the possible space groups as $P4_2/mcm$ (No. 132), $P4_2cm$ (No. 101) and $P\overline{4}\,c2$ (No. 116), as previously suggested.

Looking for a possible structural model (Kaduk, 2002) a search for binary fluorides with the ANX formula ABX_6, limited to tetragonal symmetry, was performed using the Inorganic Crystal Structure Database (© FIZ Karlsruhe, see, for example, Belsky *et al.*, 2002). This resulted in seven propositions, out of which particular attention has been paid to the $KSbF_6$ structure (Kruger *et al.*, 1976). $KSbF_6$ crystallizes in the tetragonal system, a = 5.16, c = 10.07 Å, and was initially described in the space group $P\overline{4}2m$. It was then re-examined, neglecting insignificant deviations, and redescribed as an averaged structure in the space group $P4_2/mcm$ (ICSD reference No. 42509). In the latter description, the K^+ ions occupy the 2(d) site and are surrounded by eight fluoride ions, forming trigonal dodecahedra further linked by edge sharing to form infinite $[KF_6]^{5-}$ chains. The Sb^{5+} ions occupy the 2(a) site and exhibit octahedral coordination, with isolated $[SbF_6]^-$ octahedra sharing corners with adjacent $[KF_6]^{5-}$ chains to form the three-dimensional framework. At first sight, no structural relationship could have been expected between $KSbF_6$ and $CaTbF_6$, as the tetravalent terbium is reluctant to accommodate the octahedral site occupied by the Sb^{5+} ions in $KSbF_6$. However, in fluoroterbates the eight-coordinated Tb^{4+} ions frequently adopt a trigonal dodecahedral environment.

Table 1
Experimental details.

	Neutron	X-ray
Crystal data		
Chemical formula	$CaTbF_6$	$CdTbF_6$
M_r	312.99	385.33
Cell setting, space group	Tetragonal, $P4_2/m$	Tetragonal, $P4_2/m$
a, c (Å)	5.2696 (1), 7.7105 (2)	5.18770 (2), 7.69451 (3)
V (Å^3)	214.11 (1)	207.08 (1)
Z	2	2
D_x (Mg m^{-3})	4.85	6.18
Radiation type	Thermal neutron	Cu $K\alpha$
Temperature (K)	293	293
Specimen form, colour	Cylinder, white	Flat sheet, white
Specimen preparation temperature (K)	900	830
Data collection		
Diffractometer	3T2	Phillips X-pert
Data collection method	Specimen mounting: cylindrical container; mode: reflection; scan method: step	Bragg–Brentano geometry with plane sample holder; mode: reflection; scan method: step
2θ (°)	$2\theta_{min}$ = 6, $2\theta_{max}$ = 126, increment = 0.05	$2\theta_{min}$ = 5, $2\theta_{max}$ = 140, increment = 0.012
Refinement		
Refinement on	Integrated intensities	Integrated intensities
R factors and goodness-of-fit	R_p = 0.116, R_{wp} = 0.110, R_{exp} = 0.057, S = 1.92	R_p = 0.158, R_{wp} = 0.185, R_{exp} = 0.155, S = 2.21
Wavelength of incident radiation (Å)	1.2251	1.54056
Excluded region(s)	None	None
Profile function	Pseudo-Voigt	Pseudo-Voigt
No. of parameters	9	8
Weighting scheme	$1/[Y_i + \sigma(Y_i)]$	$1/[Y_i + \sigma(Y_i)]$
$(\Delta/\sigma)_{max}$	<0.0001	<0.0001
Preferred orientation correction	None	None

Computer programs: *FULLPROF* (Rodriguez-Carvajal, 1991), *CaRIne* (C. Boudias & D. Monceau, 1989).

Table 2
Atomic coordinates and equivalent isotropic displacement parameters for the $MTbF_6$ (M = Ca, Cd) compounds from X-ray data in the space group $P4_2/m$ (italic: values refined from neutron diffraction for $CaTbF_6$).

Atoms	Sites	x	y	z	B_{eq} (Å$_2$)
$CaTbF_6$					
Ca	2(a)	0	0	1/2	1.85 (5)
	2(a)	*0*	*0*	*1/2*	*1.05 (4)*
Tb	2(f)	1/2	1/2	3/4	1.60 (2)
	2(f)	*1/2*	*1/2*	*3/4*	*−0.03 (2)*
F1	8(k)	0.214 (1)	0.256 (1)	0.3174 (4)	2.25 (8)
	8(k)	*0.2103 (2)*	*0.2550 (2)*	*0.3184 (1)*	*1.54 (2)*
F2	4(j)	0.352 (2)	0.683 (2)	1/2	2.25 (8)
	4(j)	*0.3440 (4)*	*0.6769 (4)*	*1/2*	*1.18 (3)*
$CdTbF_6$					
Cd	2(a)	0	0	1/2	1.67 (4)
Tb	2(f)	1/2	1/2	3/4	1.39 (4)
F1	8(k)	0.200 (1)	0.262 (1)	0.3224 (4)	2.1 (1)
F2	4(j)	0.351 (3)	0.693 (3)	1/2	2.1 (1)

Then the possibility of $CaTbF_6$ crystallizing with an '*anti*-$KSbF_6$' structure, in which the Tb^{4+} ions would be substituted for the K^+ ions and the Ca^{2+} ions occupy the octahedral site, was envisaged.

Rietveld refinement (from X-ray data) of the crystal structure of $CaTbF_6$, using an '*anti*-$KSbF_6$' structural model derived from the description of the structure in the space group $P4_2/mcm$, was performed and rapidly converged to acceptable agreement factors. However, neutron diffraction data were used to prevent lowering of the possible symmetry of the anionic sublattice, which is virtually undetectable in X-ray patterns in the presence of heavy X-ray scatterers.

The Rietveld refinement of the neutron diffraction pattern of $CaTbF_6$ using the $P4_2/mcm$ description immediately revealed that the space-group assignment was incorrect. Numerous reflections incorrectly included, such as 120, 123 or 230 and the unambiguous presence of the 033 reflection which are undetected in the X-ray powder diffraction pattern, definitively ruled out the space group $P4_2/mcm$, which requires $0kl$ reflections with $l = 2n$, and suggested the possible space groups $P4_222$ (No. 93), $P4_2/m$ (No. 84) and $P4_2$ (No. 77). As the distortion arises from the anionic sublattice, the space group $P4_2$, which implyies an extra degree of freedom for the cationic lattice along the c axis, was *a priori* inconsistent and definitively excluded later by attempted refinements which did not improve the results significantly. Of the two remaining space groups, $P4_222$ is unlikely, because of the necessity to describe one of the two independent F atoms using the 4(o) site. This 'x, x, 1/4' site, apart from requiring a translated origin, does not provide the supplementary degree of freedom expected for this independent atom and rejection of this group was confirmed by subsequent refinements. Thus, $CaTbF_6$ was redescribed in the space group $P4_2/m$, which keeps the cationic positions unchanged but provides the anionic sublattice with the necessary additional degree of freedom. Fig. 1 displays the final fit between calculated and observed neutron diffraction patterns and Table 1 summarizes the details of the final Rietveld refinement of the $CaTbF_6$ crystal structure, from X-ray and neutron powder diffraction data. Fig. 2 displays the final plot of the Rietveld refinement from X-ray data.[1]

Table 2 shows good agreement between the atomic coordinates obtained from both X-ray and neutron data. More-

[1] Supplementary data for this paper are available from the IUCr electronic archives (Reference: AV5017). Services for accessing these data are described at the back of the journal.

Table 3
Important bond lengths (Å) for $CaTbF_6$ and $CdTbF_6$.

Tb^{IV} polyhedron [CN 8] dodecahedral	M^{II} (M = Ca, Cd) polyhedron [CN 6] octahedral
$CaTbF_6$	
Tb—F1$^{i, ii, iii, iv}$: 2.066 (1) × 4	Ca—F1$^{vii, viii, ix, x}$: 2.236 (1) × 4
Tb—F2$^{i, iii, v, vi}$: 2.294 (1) × 4	Ca—F2$^{i, xi}$: 2.488 (2) × 2
$d\langle$Tb—F$\rangle$ = 2.180	$d\langle$Ca—F$\rangle$ = 2.320
d_{th} = 2.162	d_{th} = 2.248
$CdTbF_6$	
Tb—F1$^{i, ii, iii, iv}$: 2.066 (7) × 4	Cd—F1$^{vii, viii, ix, x}$: 2.187 (7) × 4
Tb—F2$^{i, iii, v, vi}$: 2.303 (8) × 4	Cd—F2$^{i, xi}$: 2.419 (14) × 2
$d\langle$Tb—F$\rangle$ = 2.184	$d\langle$Cd—F$\rangle$ = 2.264
d_{th} = 2.162	d_{th} = 2.217

Symmetry codes: (i) x, y, z; (ii) $-y, x, \frac{1}{2}-z$; (iii) $1-x, 1-y, z$; (iv) $y, 1-x, \frac{1}{2}-z$; (v) $1-y, x, \frac{1}{2}+z$; (vi) $y, 1-x, \frac{1}{2}+z$; (vii) $1-x, -y, -z$; (viii) $1+x, y, -z$; (ix) $1-x, -y, z$; (x) $-1+x, y, -z$; (xi) $-x, -y, z$.

over, the slight distortion of the anionic sublattice (inducing a space-group change from $P4_2/mcm$ to $P4_2/m$) is confirmed. The x and y coordinates of the F atoms are also clearly differentiated from the 'x, x' and '$x, -x$' coordinates encountered in the $P4_2/mcm$ description when refined from X-ray data. It is worth noticing that there was no evidence for symmetry lowering related to the anionic sublattice in the starting refinement performed in the space group $P4_2/mcm$ from X-ray data. The interatomic distances obtained from neutron diffraction data confirm the accuracy of the structural parameters between the two F2 atoms involved in edge sharing between the $[TbF_8]^{4-}$ polyhedra, as shown by the important bond lengths displayed in Table 3 and the shortest F—F distance (2.486 Å) encountered in the polyhedral string.

Starting from the results obtained for $CaTbF_6$, the crystal structure of $CdTbF_6$ was investigated by X-ray powder diffraction. It should be noted that for both $CaTbF_6$ and $CdTbF_6$, a significant asymmetry of some diffraction peak particulars was observed. This is probably due to the superposition of the contributions of structure particulars to instrumental aberrations and the size effects generally responsible for the asymmetry. Details of the final Rietveld refinement of $CdTbF_6$ structure are summarized in Table 1. Fig. 3 shows the final Rietveld plot of both observed and calculated patterns. The $[TbF_8]^{4-}$ dodecahedra are almost unaffected by the substitution of cadmium for calcium and the polyhedral string is only tightened in order to accommodate the smaller Cd^{2+} cation, which requires shorter M^{II}—F distances (Table 3).

Although the structural relationship between the $MTbF_6$ (M = Ca, Cd) fluorides and $KSbF_6$ is in some way surprising, the bond-valence analysis performed according to the method of Brese & O'Keeffe (1991) displayed in Table 4 unambiguously confirms the adequacy of the *anti*-$KSbF_6$ structural model. The excellent agreement between expected and calculated values for the valence of the Tb^{4+} ions and the similarity of their environment indicate that terbium prevails in the polyhedral string. The divalent cations accommodated in octahedral sites in the interchain space ensure the electrical neutrality and the cohesion of the three-dimensional framework.

4. Description of the structure and discussion

Both $CaTbF_6$ and $CdTbF_6$ are characterized by dodecahedral eight-coordination of the Tb^{4+} ions. By sharing opposite and orthogonal edges involving F2—F2 contacts the $[TbF_8]^{4-}$ dodecahedra form infinite $[TbF_6]^{2-}$ chains extending along the c axis. These chains are further linked by sharing corners with isolated $[MF_6]^{4-}$ octahedra to form the three-dimensional framework (Figs. 4*a* and *b*). More accurately, each $[MF_6]^{4-}$ octahedron shares its equatorial vertices involving F1 atoms exclusively with four adjacent dodecahedra belonging to two opposite $[TbF_6]^{2-}$ chains. The two remaining F2 apical vertices belong to two other alternate chains and are involved in edge sharing between $[TbF_8]^{4-}$ dodecahedra. These apical F2 atoms point towards the $\langle 110 \rangle$ direction.

Although rather astonishing, the interrelationship between the $MTbF_6$ (M = Ca, Cd) and $KSbF_6$ fluorides shows that the anionic packing involved in this structural type may accommodate several different charge combinations. Apparently, a significant variety of cations might be incorporated into this structure. This high tolerance is

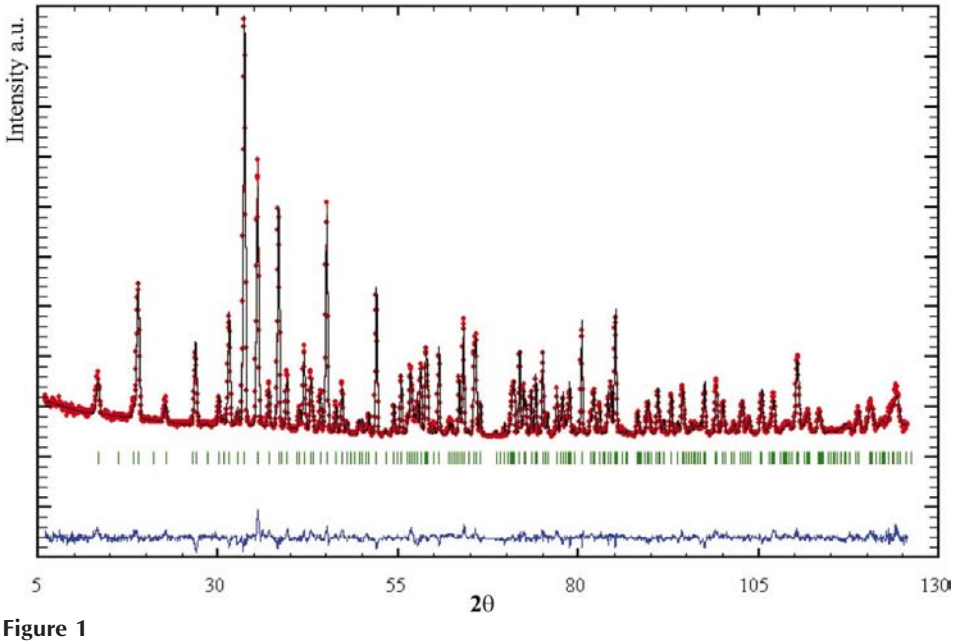

Figure 1
Final Rietveld plot of $CaTbF_6$ from neutron powder diffraction data: observed (filled circles) and calculated (solid line) patterns, difference pattern (observed minus calculated, lower solid line) and Bragg reflections (vertical markers).

reflected in the spread of cell edges and the corresponding *c*/*a* ratios: 1.95 for $KSbF_6$, 1.46 ($CaTbF_6$), 1.49 ($CdTbF_6$) and 1.68 ($NaSbCl_6$).

Thus, from $KSbF_6$ through to $CaTbF_6$ the *a* parameter does not change by more than 2.1%, while the *c* parameter decreases by *ca* 23.5%. The *c* parameter seems to be directly governed by the size of the cation in eightfold coordination within the infinite $[M^xF_6]^{(6-x)-}$ chain of edge-sharing dodecahedral groups, as well as its capability to introduce more or less covalency in the ionic bond. Let us consider the polyhedral string lying in the average ⟨110⟩ planes of both $KSbF_6$ and $CaTbF_6$ structures, as displayed in Fig. 5. Fig. 5(*a*) has been drawn from data issued from the re-description of the structure of $KSbF_6$ in the more symmetrical space group $P4_2/mcm$ given in the ICSD database under the collection code 42509.

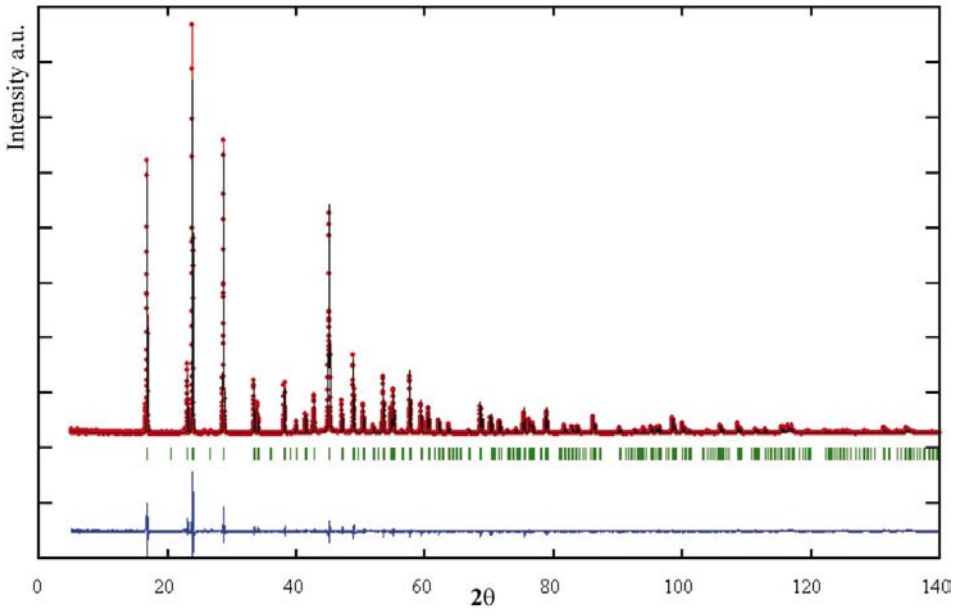

Figure 2
Final Rietveld plot of $CaTbF_6$ from X-ray powder diffraction data: observed (filled circles) and calculated (solid line) patterns, difference pattern (observed minus calculated, lower solid line) and Bragg reflections (vertical markers).

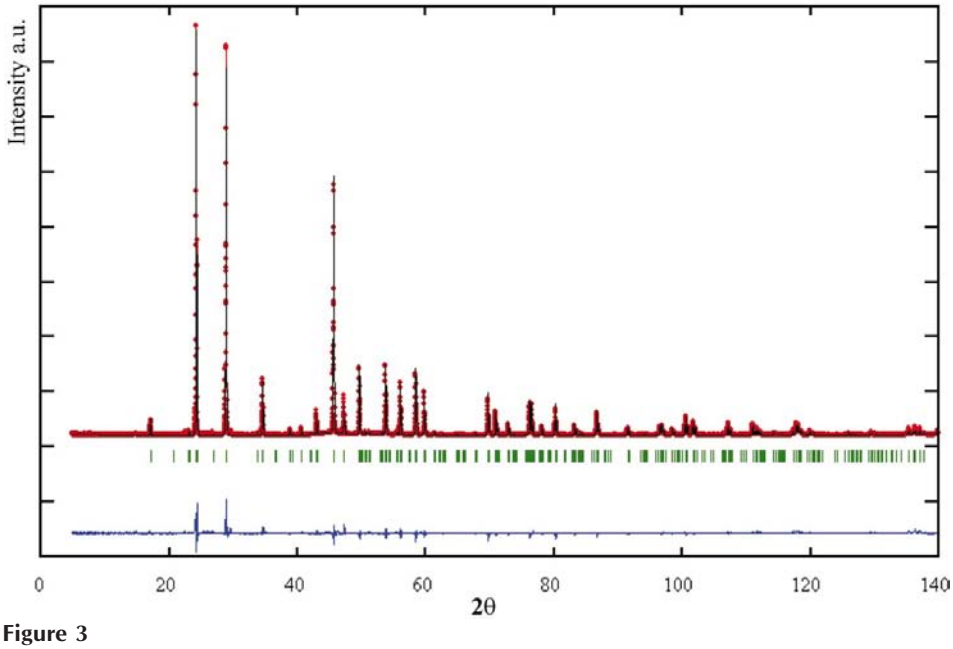

Figure 3
Final Rietveld plot of $CdTbF_6$ from X-ray powder diffraction data: observed (filled circles) and calculated (solid line) patterns, difference pattern (observed minus calculated, lower solid line) and Bragg reflections (vertical markers).

Traditionally the dodecahedral eight-coordination (dodecahedron or bisdisphenoïd) may be considered as consisting of two interpenetrating tetrahedra (disphenoïd), elongated *A* and flattened *B* (Wells, 1975). These two tetrahedra are characterized by θ_A and θ_B angles, respectively, which are the half-angles between bonds.

For the idealized $\bar{4}2m$ point symmetry of the most regular dodecahedron (hard-sphere model) the θ_A and θ_B angles are equal to 36 and 69°, respectively, whereas θ_B rises to 72° in the ligand–ligand energy-repulsion approach (electrostatic model; Wells, 1975).

With this description in mind one can see that for both $KSbF_6$ and $CaTbF_6$ structures the *c* parameter depends directly on the geometry of the tetrahedra. In the $[KF_8]^{7-}$ dodecahedron the $A-X$ and $B-X$ distances are respectively equal to 3.0958 and 2.6369 Å. In the $[TbF_8]^{4-}$ dodecahedron the corresponding distances are equal to 2.2936 and 2.0677 Å. Although the dodecahedra in $KSbF_6$ and $CaTbF_6$ are not similar, it is worth noticing that the ratio of the $A-X$ distances within the dodecahedral groups (1.351) is close to the ratio of the unit-cell parameters (*c*) of these structures (1.306), whereas the ratio of the corresponding ionic radii, $r_{K^+}/r_{Tb^{4+}}$ = 1.633, is higher. The θ_A/θ_B ratio is now equal to 0.53 for incompressible atoms (hard-sphere model) and 0.51 for the electrostatic model. Taking this ratio as a measure of the distortion of the anionic packing, one can see that the distortion is much more important in $[TbF_8]^{4-}$, where θ_A/θ_B = 0.423, than in the $[KF_8]^{7-}$ dodecahedron (θ_A/θ_B = 0.574). A deeper examination of the variations of both the characteristic

Table 4
Bond-valence analysis of the structures of $CaTbF_6$ (from neutron data) and $CdTbF_6$ (from X-ray data).

		$CaTbF_6$			$CdTbF_6$		
	v_{th}	F1	F2	v_{ex}	F1	F2	v_{ex}
M^{II}	2	4 × 0.345	2 × 0.174	1.728	4 × 0.362	2 × 0.194	1.836
Tb^{IV}	4	4 × 0.649	4 × 0.351	4.000	4 × 0.649	4 × 0.342	3.964
Anionic coordination		Ca	Ca		Cd	Cd	
		Tb	2 Tb		Tb	2 Tb	
v_{ex} (v_{th} = 1)		0.994	0.876		1.011	0.878	

angles θ_A and θ_B of the dodecahedra (Table 5) shows that the flattening of the *B* tetrahedron is the predominant deformation accounting for the important reduction of the *c* parameter while going from $KSbF_6$ to $CaTbF_6$. However, as the value of the θ_A angle is lower than 35.60° for the $[TbF_8]^{4-}$ dodecahedron, this polyhedron is much more elongated than that of $[KF_8]^{7-}$. This accounts for the fact that the *c* parameter of $CaTbF_6$ is not as short as expected from the ratio of the ionic radii.

On the other hand, if the *a* parameter does not change significantly it is because there is compensation between the bond-length increase and the decrease in octahedral and dodecahedral groups, respectively. To illustrate this assumption the averaged bond lengths in octahedral and dodecahedral groups were calculated using the bond-valence parameters recommended by Brese & O'Keeffe (1991) and those suggested by Gaumet *et al.* (1997) for Tb^{4+}. This calculation resulted in values equal to 2.76 and 2.16 Å for K^+ and Tb^{4+} in a dodecahedral environment, and 1.87 and 2.35 Å for Sb^{5+} and Ca^{2+} in octahedral groups, respectively. This represents a reduction of 21.7% of the average distance in dodecahedral sites and an increase of 25.7% of this distance in the octahedral sites. The compensation mechanism accounting for the variation in the *a* parameter can be understood by considering the variation of representative distances parallel to ⟨110⟩, such as the F2—F2 edge in the $[MF_8]$ dodecahedron and the F1—F1 edge in the $[MF_6]$ octahedron. While the latter is equal to 3.60 and 2.49 Å in $KSbF_6$ and $CaTbF_6$, respectively (*i.e.* a reduction of 30.8%), the former is equal to 2.64 and 3.49 Å (*i.e.* an increase of 32.2%), corresponding to a global increase of the typical distances encountered parallel to ⟨110⟩, *i.e.* a slight increase in the *a* parameter. In the present considerations the lowering of the space-group symmetry from $P4_2/mcm$ to $P4_2/m$, which makes the previous distances independent and minimizes their influence on the *a* parameter, has not been accounted for, while the flattening of the dodecahedral environment leads to an additional increase of the *a* parameter.

For chains built of edge-sharing dodecahedra another distance of interest is the separation between the two nearest corners on both sides of the shared edges, *i.e.* distance *d* on Fig. 5. Elementary calculations show that distance *d* may be approximated by the following relation

$$d = 2(M-X)(\cos\theta_A - \cos\theta_B)(A-X)/(B-X),$$

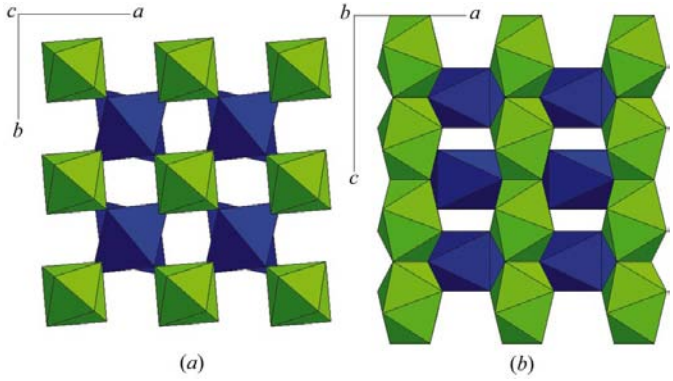

Figure 4
Projections of the crystal structure of $CaTbF_6$ along (*a*) [001] and (*b*) [010].

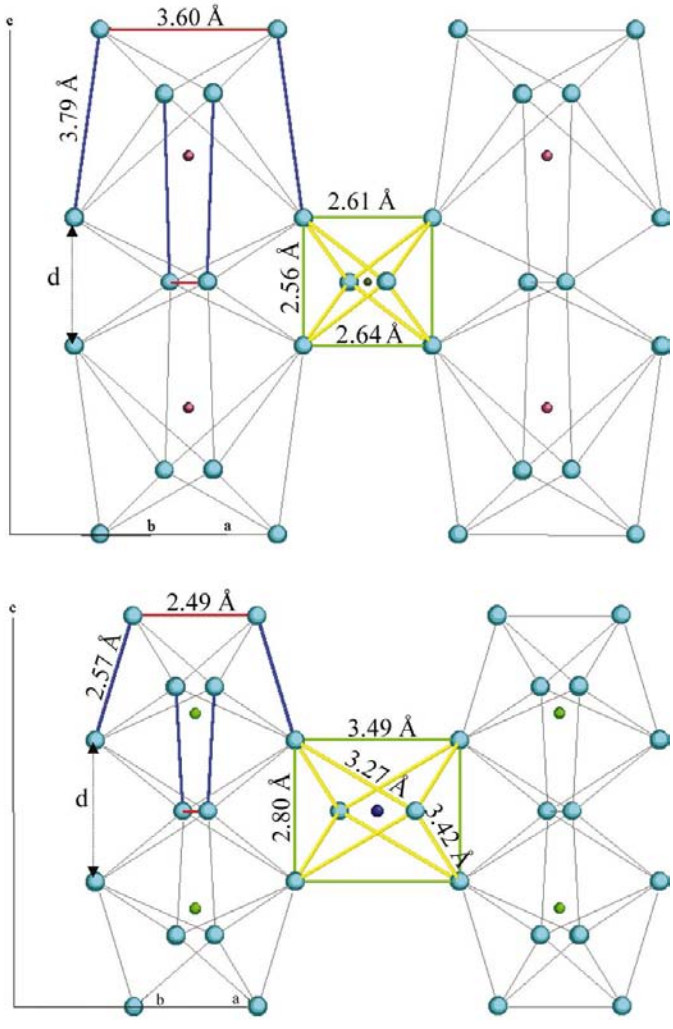

Figure 5
Evolution of the polyhedra shapes in the transition from (*a*) $KSbF_6$ to (*b*) $CaTbF_6$ (scale is respected between *a* and *b*).

Table 5
Evolution of the $[MF_8]$ dodecahedra in $KSbF_6$, $CdTbF_6$ and $CaTbF_6$ structures with respect to the Hard Sphere (HS) and Electrostatic (El) models, showing that the flattening prevails ($\Delta\theta_B > \Delta\theta_A$).

	$KSbF_6$	$CdTbF_6$	$CaTbF_6$
θ_A (°)	35.6	33.3	32.8
$\Delta\theta_A$ (%) HS-El	7.9	13.7	15.1
$\Delta\theta_A$ (%) $KSbF_6$	–	5.9	7.2
θ_B (°)	62.0	74.4	75.2
$\Delta\theta_B$ (%) HS	−10.7	7.1	8.3
$\Delta\theta_B$ (%) $KSbF_6$	–	17.2	19
$\Delta\theta_B$ (%) El	−13.9	3.3	4.5
$\Delta\theta_B$ (%) $KSbF_6$	–	17.2	18.1

where $M-X$ is the mean bond length in the dodecahedron and $A-X$ and $B-X$ are the bond lengths in the elongated and flattened interpenetrating tetrahedra, respectively.

The more elongated the A tetrahedron and the more flattened the B one, the longer the d distance. Despite the smaller size of the $[TbF_8]^{4-}$ dodecahedron compared with that of $[KF_8]^{7-}$, the deformation (strong elongation of the bonds but flattening of this polyhedron) of the former results in an increase of the distance from 2.56 to 2.80 Å. This distance represents an equatorial edge of the octahedron linking the chains together and encompassing the Ca^{2+} cations, and for an ideal bond length of 2.35 Å the length of the edges for a regular octahedron should be 3.32 Å. Therefore, the constrained distance of 2.80 Å encountered in the $[CaF_6]^{4-}$ octahedron accounts for the fact that in $CaTbF_6$ the deformation of the anionic sublattice is controlled by the Tb^{4+} ions. On the contrary, the more regular octahedron surrounding the Sb^{5+} ion in $KSbF_6$ shows that this ion controls the distortion of the anionic sublattice.

It is worth noting that $NaSbCl_6$ also crystallizes in the tetragonal symmetry (Henke, 1992) with a unit cell similar to that of $KSbF_6$ and this $NaSbCl_6$ structure is described in the space group $P4_2/m$. However, despite the similarities of their unit cells and their common space group ($P4_2/m$, No. 84), the polyhedral linkages of $CaTbF_6$ and $NaSbCl_6$ are different. Both $CaTbF_6$ and $NaSbCl_6$ structures are built of infinite chains of edge-sharing dodecahedral groups arranged in a tetragonal packing. Whereas these chains are linked together by isolated octahedra sharing only corners in $CaTbF_6$ they are joined by isolated octahedra sharing edges with dodecahedral groups in $NaSbCl_6$. The structure of $KSbF_6$ may be related to that of $NaSbCl_6$ by interchanging the occupied and unoccupied octahedral holes (Sb sites) of the anionic sublattice (Fig. 6). From the viewpoint of crystal chemistry, this corresponds to the displacement vectors $\mathbf{t}_1 = [\frac{1}{2}\ 0\ 0]$ and $\mathbf{t}_2 = [0\ \frac{1}{2}\ 0]$ applied to Sb atoms located at $z = 0$ and $z = 1/2$, respectively, in $NaSbCl_6$ followed by a translation of the origin $\mathbf{t} = (\frac{1}{2}\ \frac{1}{2}\ 0)$.

In hexahalides such as $KSbF_6$, $CaTbF_6$ or $NaSbCl_6$, the halide ion sublattice (Peresypkina & Blatov, 2003, and references therein) is the structure-forming one. As these sublattices are not strictly close-packed arrangements they may undergo strong distortions depending on the size, the charge and the covalency effects of the counter-cations. Thus, starting from a simple cubic fluoride-ion arrangement where all the voids are regular cubes, the distortion of the anionic sublattice (considering a body-centered cationic sublattice) may be regarded as resulting from the transformation of one cubic site out of two into a dodecahedral environment. The transformation of a regular cube into a dodecahedron proceeds from the elongation of one of the two tetrahedra included in the cube and the compression of the other along the direction of one of the quaternary axes. This results in a lowering of the symmetry from cubic ($m3m$) to tetragonal ($\bar{4}2m$) and of course the two opposite edges of the elongated tetrahedra perpendicular to the quaternary axis are orthogonal. By applying this transformation to all the separate cubes in the columns parallel to the quaternary axis (Fig. 7) and surrounding an identical column of isolated cubes, in such a way that the elongated tetrahedra alternate from one cube to the next one, results in parallel edges between two adjacent dodecahedra merging into shared edges. This mechanism results in the formation of infinite chains of edge-sharing dodecahedra and in the elimination of two fluoride ions per isolated cube in the central column, leading to a distorted octahedral environment linking the chains. This architecture is the basic polyhedral linking of both $KSbF_6$ and $CaTbF_6$ structures. Depending on the nature and the charge (and therefore the size) of the counter-cations through their covalency effect, it is either the dodecahedral or the octahedral cationic environments which are close packed. Thus, in $KSbF_6$ the most charged cation, Sb^{5+}, occupies the octahedral site of the closest packing of fluoride ions, whereas the K^+ ions lie in the dodecahedral interstices. On the contrary, the structure of $CaTbF_6$ may be described as close-packed assemblies of Tb^{4+} and F^- ions, in which the Ca^{2+} ions occupy octahedral holes of the anionic sublattice.

The fact that $CaTbF_6$ and $CdTbF_6$ crystallize with an *anti*-$KSbF_6$ structure rather than an *anti*-$NaSbCl_6$ structure may be

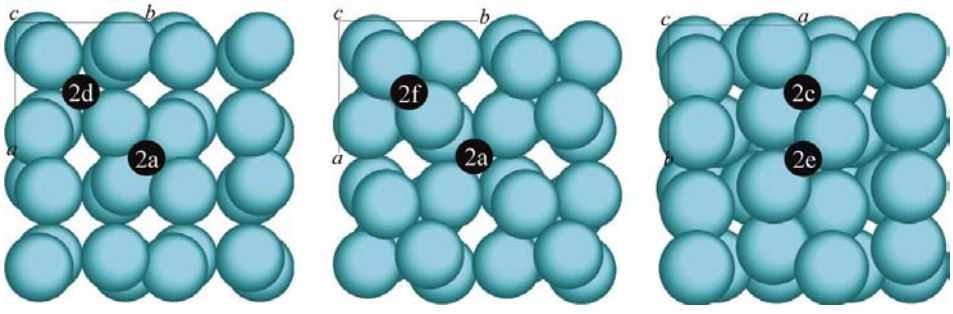

Figure 6
Dodecahedral and octahedral interstices within the anionic packing of $KSbF_6$ ($P4_2/mcm$, left), $CaTbF_6$ ($P4_2/m$, center) and $NaSbCl_6$ ($P4_2/m$, right).

understood by comparing the size of the unoccupied octahedral hole in $NaSbCl_6$, which is greater than that of the occupied hole due to the Cl—Cl contact distances around the former. In fact, both $CaTbF_6$ and $CdTbF_6$ structures have been described with an octahedral coordination of Ca and Cd atoms for convenience. This corresponds to the first coordination sphere composed of four F atoms at 2.236 Å and two at 2.488 Å, but there are four additional fluoride ions at 3.01 Å which belong to the absolute coordination of the calcium which is thus 6 + 4. It may also be argued that these four additional F atoms are too far away to be bonded and therefore to be considered in the coordination sphere of the larger cation, justifying the *anti*-$KSbF_6$ description of this structure.

This 6 + 4 environment can be correlated to the crystal structure of β-$BaTbF_6$ (Largeau *et al.*, 1997), where a true ten-coordination of the Ba^{2+} ions occurs. This structure, as well as that of the title compounds, is characterized by a tetragonal packing of the infinite $[TbF_6]^{2-}$ chains of edge-sharing $[TbF_8]^{4-}$ dodecahedra, but the tetragonal symmetry breaks down in favour of the orthorhombic one. This leads to a small variation in the distances between adjacent chains which are equal to 5.52 and 5.75 Å along [001] and [010], respectively, and significantly greater than the corresponding distances in $CaTbF_6$ or $CdTbF_6$, *i.e.* 5.27 or 5.19 Å, respectively. The increase in distances between nearest chains results from the increase of the corresponding *a* and *b* parameters, and proceeds from the augmentation of the size of the divalent cation, whereas the unit-cell parameter in the third direction characteristic of the $[TbF_6]^{2-}$ chain sequence remains unchanged, *i.e.* 7.76 Å for β-$BaTbF_6$ against 7.71 and 7.70 Å for $CaTbF_6$ and $CdTbF_6$, respectively. The accommodation of the larger Ba^{2+} ions requires a rotation of $\pi/2$ of successive chains relative to each other along the *b* axis, accounting for the doubling of this cell parameter and resulting in the appearance of the orthorhombic symmetry.

Fig. 8 displays the structure field map of some $A^{2+}B^{4+}F_6$ fluorides. Apart from the fluoroterbates, compounds gathered in this map are divided into three major families, namely the $LiSbF_6$ type (Burns, 1962), the $NaSbF_6$ type (Teufer, 1956) and the disordered tysonite type (Babel & Tressaud, 1985).

In the two former structural types both A^{2+} and B^{4+} lie in octahedral environments, whereas in the disordered tysonite stabilized for tetravalent cations of larger size both A^{2+} and B^{4+} cations are nine-coordinated. From the viewpoint of crystal chemistry mostly governed by ionic radii and taking into account that the ionic radius of Tb^{4+} is intermediate between those of Zr^{4+} and Pb^{4+} (for a given coordination), the $CdTbF_6$ compound could have been expected to crystallize with the $LiSbF_6$ structure within a homogeneous $CdM^{4+}F_6$ series ($CdZrF_6$: Babitsyna *et al.*, 1989). For the same reasons the $CaTbF_6$ compound could have been expected to exhibit the $NaSbF_6$-type structure. The fact that both $CdTbF_6$ and $CaTbF_6$ fluorides adopt an *anti*-$KSbF_6$ structure clearly illustrates the preference of the Tb^{4+} ion for eight coordination. However, the general trend expected when going from one structure field to the other (*i.e.* the larger the ionic radius, the higher the coordination number) is fulfilled, as shown by Fig. 8. The structures of both $CdM^{4+}F_6$ and $CaM^{4+}F_6$ families change from the $LiSbF_6$ and $NaSbF_6$ types, respectively, towards disordered tysonite ($CdThF_6$: Keller & Salzer, 1967) when the size of the M^{4+} cation increases. For both Cd and Ca families the structural change occurs for an ionic radius of the M^{4+} cation

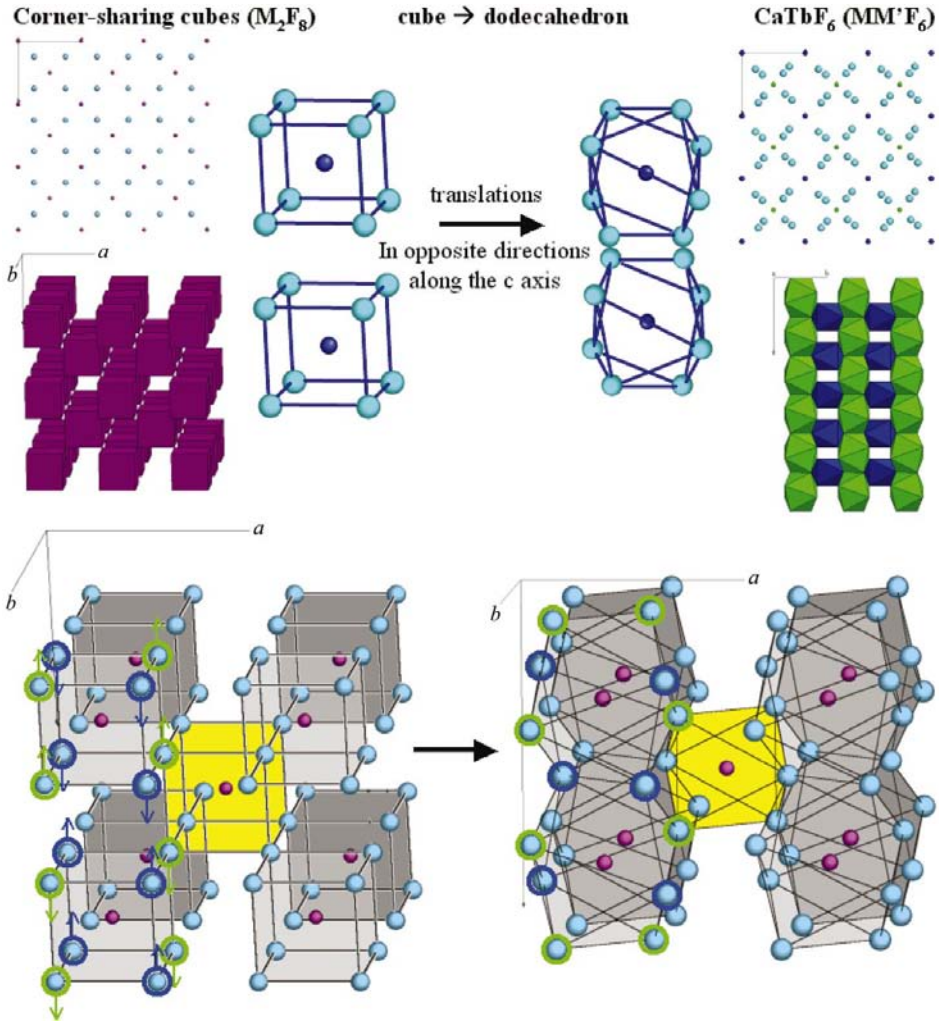

Figure 7
Relationship between the cubic fluoride-ion arrangement and the anionic sublattices of title compounds.

(in six-coordination) greater than 0.92 Å, *i.e.* beyond Pb^{4+} in the map of Fig. 8. This change of structure is accompanied by a sudden rise of the M^{4+} coordination from 6 to 9. As the Tb^{4+} ion in both $CdTbF_6$ and $CaTbF_6$ is found in eight-coordination with the corresponding value of its ionic radius equal to 1.02 Å, the representative points of these structures are logically located at the border field between the octahedral and the nine-coordination of the M^{4+} cations, where they were not expected. Therefore, the *anti*-$KSbF_6$ structure type is a consistent intermediate between structural types based on six- or nine-coordination of the tetravalent ions. It appears that

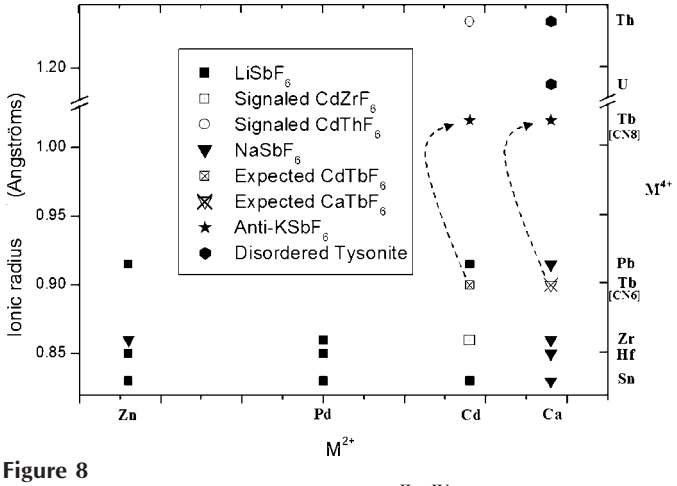

Figure 8
Composite structure field map for some $M^{II}M^{IV}F_6$ fluorides.

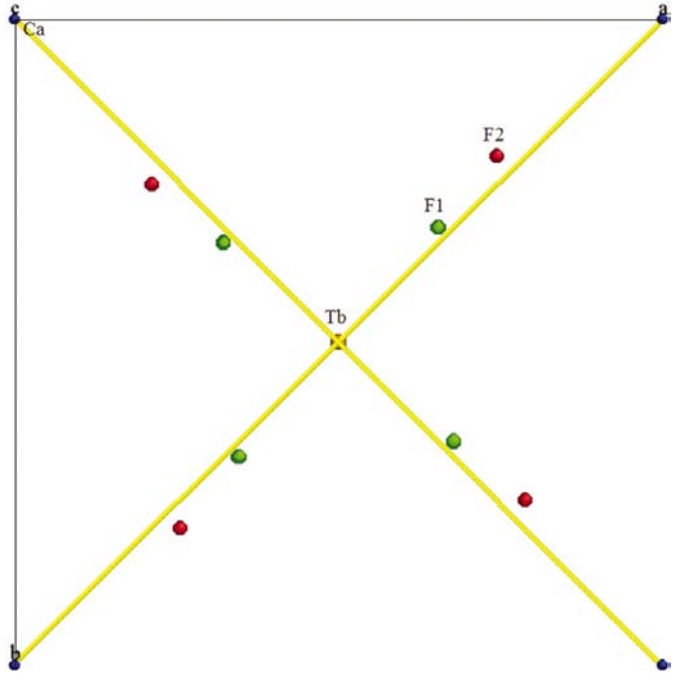

Figure 9
Projection of the structure of $CaTbF_6$ onto the (001) plane showing the relaxation of the anionic sublattice, thus assigning the description of this structure to the $P4_2/m$ space group (in the $P4_2/mcm$ space group of the $KSbF_6$ parent structure the anions lie on the *c* mirrors).

factors other than the ionic size are involved here: possibly the Tb^{4+} ion having special covalent bonding requirements due to its half-filled $4f^7$ electronic configuration, which leads to singular structural types. Thus, the predilection of the Tb^{4+} ion for the eight-coordination explains the departure of these compounds from their expected $LiSbF_6$ and $NaSbF_6$ homogeneous structural families.

It is also worth noting that the dodecahedral eight-coordination with $\overline{4}$ point symmetry has already been encountered several times in the crystal chemistry of the Tb^{4+} ion, namely in KTb_3F_{12} (Largeau *et al.*, 1998), Li_2CaTbF_8 (Largeau, 1998) and Cd_2TbF_8 (Largeau & El-Ghozzi, 1998). In all these structures there is only one crystallographically independent Tb^{4+} ion and in both Li_2CaTbF_8 and Cd_2TbF_8, where the dodecahedral $[TbF_8]^{4-}$ groups are isolated from each other, the eight-coordination is almost undistorted with θ_A/θ_B ratios equal to 0.558 and 0.503, respectively. On the contrary in KTb_3F_{12}, where infinite $[TbF_6]^{2-}$ chains are present, the $[TbF_8]^{4-}$ dodecahedron exhibits a shape very similar to that encountered in $CaTbF_6$ with a mean bond length equal to 2.17 Å, $\theta_A = 32.26$ and $\theta_B = 75.42^\circ$, resulting in a θ_A/θ_B ratio equal to 0.428. The dodecahedral eight-coordination is also observed in the quenchable high-temperature form β-$BaTbF_6$. Contrary to the preceding groups, the dodecahedral group exhibits the local symmetry 222 rather than $\overline{4}$. However, a careful examination of the dodecahedron surrounding the Tb^{4+} ion shows that this environment is quite similar to those of $CaTbF_6$ or KTb_3F_{12} with a mean bond length of 2.176 Å and a θ_A/θ_B ratio equal to 0.401. These observations and the slight distortion observed in the title compounds (Fig. 9), which are unpredictable and unjustified considering either the cationic or anionic sublattices, suggest that the apparent preference of the Tb^{4+} ion for the $\overline{4}$ point symmetry may be another outstanding feature of the singular crystal-chemical behavior of fluoroterbates.

5. Conclusion

The original *anti*-$KSbF_6$ structures of both $CaTbF_6$ and $CdTbF_6$ fluorides have been solved and refined by taking advantage of powder X-ray and high-resolution neutron diffraction complementarities. Correlations between the anionic sublattices of $CaTbF_6$, $CdTbF_6$, $KSbF_6$ and $NaSbCl_6$ and a simple cubic fluoride-ion arrangement have been established. The unexpected position of the title compounds within a representative $M^{2+}M^{4+}F_6$ structure field map emphasizes the peculiar crystal chemistry of these two new tetravalent terbium fluorides. This suggests that the Tb^{4+} ion would be systematically expected to be in eight-coordination in a fluorinated environment and confirms that this singular behavior of the Tb^{4+} ion in fluorides would be ascribable to its half-filled $4f^7$ electronic configuration rather than to its ionic radius.

Further developments of the crystal-chemical properties of fluoroterbates are currently in progress in order to determine the outstanding criteria governing this singular crystal chemistry.

The authors are very indebted to F. Bourée (Laboratoire Léon Brillouin, Saclay, France) for recording the high-resolution neutron patterns.

References

Babel, D. & Tressaud, A. (1985). *Inorganic Solid Fluorides, Chemistry and Physics*, edited by P. Hagenmuller, Ch. 3, pp. 77–203. New York: Academic Press.

Babitsyna, A. A., Emel'yanova, T. A. & Chernov, A. P. (1989). *Zh. Neorg. Khim.* **34**, 3145–3149.

Belsky, A., Hellenbrandt, M., Lynn, V., Luksch, K. & Luksch, P. (2002). *Acta Cryst.* B**58**, 364–369.

Boultif, A. & Louër, D. (1991). *J. Appl. Cryst.* **24**, 987–993.

Brese, N. E. & O'Keeffe, M. (1991). *Acta Cryst.* B**47**, 192–197.

Burns, J. H. (1962). *Acta Cryst.* **15**, 1098–1101.

El-Ghozzi, M. & Avignant, D. (2001). *J. Fluor. Chem.* **107**, 229–233.

Feldner, K. & Hoppe, R. (1983). *Rev. Chim. Miner.* **20**, 351–367.

Finney, J. L. (1995). *Acta Cryst.* B**51**, 447–467.

Gaumet, V., Largeau, E. & Avignant, D. (1997). *Eur. J. Solid State Inorg. Chem.* **34**, 1075–1084.

Guillot, M., El-Ghozzi, M., Avignant, D. & Ferey, G. (1992). *J. Solid State Chem.* **97**, 400–404.

Henke, H. (1992). *Z. Kristallogr.* **192**, 1–16.

Hurst, H. J. & Taylor, J. C. (1970*a*). *Acta Cryst.* B**26**, 417–421.

Hurst, H. J. & Taylor, J. C. (1970*b*). *Acta Cryst.* B**26**, 2136–2137.

Josse, M., Dubois, M., El-Ghozzi, M. & Avignant, D. (2003). *Solid State Sci.* **5**, 1141–1148.

Josse, M., Dubois, M., El-Ghozzi, M. & Avignant, D. (2005). *Solid State Sci.* In the press.

Kaduk, J. (2002). *Acta Cryst.* B**58**, 370–379.

Keller, C. & Salzer, M. (1967). *J. Inorg. Nucl. Chem.* **29**, 2925–2934.

Kruger, G. J., Pistorius, C. W. F. T. & Heyns, A. F. (1976). *Acta Cryst.* B**32**, 2916–2918.

Largeau, E. (1998). University thesis, Clermont-Ferrand, France.

Largeau, E. & El-Ghozzi, M. (1998). *J. Fluor. Chem.* **89**, 223–228.

Largeau, E., El-Ghozzi, M. & Avignant, D. (1998). *J. Solid State Chem.* **139**, 248–258.

Largeau, E., El-Ghozzi, M., Metin, J. & Avignant, D. (1997). *Acta Cryst.* C**53**, 530–532.

Peresypkina, E. V. & Blatov, V. A. (2003). *Acta Cryst.* B**59**, 361–377.

Rodriguez-Carvajal, J. (1991). Abstracts of the Satellite Meeting on Powder Diffraction of the XVth Congress of the IUCr, Toulouse, France, p. 127.

Roisnel, T., Rodriguez-Carvajal, J., Pinot, M., André, G. & Bourée, F. (1994). *Mater. Sci. Forum*, **166**, 245–250.

Teufer, G. (1956). *Acta Cryst.* **9**, 539–540.

Wells, A. F. (1975). *Structural Inorganic Chemistry*, pp. 68–69. Oxford University Press.